

## ORIGINAL ARTICLE

# Dynamic magnetic resonance sialography as a new diagnostic technique for patients with Sjögren's syndrome

Y Morimoto<sup>1</sup>, M Habu<sup>2</sup>, T Tomoyose<sup>2</sup>, K Ono<sup>3</sup>, T Tanaka<sup>1</sup>, I Yoshioka<sup>2</sup>, K Tominaga<sup>2</sup>, Y Yamashita<sup>2</sup>, T Ansai<sup>4</sup>, S Kito<sup>1</sup>, S Okabe<sup>1</sup>, T Takahashi<sup>2</sup>, T Takehara<sup>4</sup>, J Fukuda<sup>2</sup>, K Inenaga<sup>3</sup>, T Ohba<sup>1</sup>

Departments of <sup>1</sup>Oral Diagnostic Science, <sup>2</sup>Oral and Maxillofacial Surgery, <sup>3</sup>Biosciences and <sup>4</sup>Health Promotion, Kyushu Dental College, Kitakyushu, Japan

**OBJECTIVE:** To evaluate the clinical utility of dynamic magnetic resonance (MR) sialographic images as a diagnostic tool for patients with Sjögren's syndrome.

**METHODS:** The morphological findings and various kinds of functional parameters in volunteers on dynamic MR sialographic images were compared with those in five patients with definite Sjögren's syndrome.

**RESULTS:** On the MR sialographs of all five patients with Sjögren's syndrome, the so-called 'apple-tree appearance' was seen. The difference in two functional parameters using the dynamic MR sialographic data was elucidated between the two groups. The maximum area of the detectable ducts in the group of patients was significantly smaller ( $P < 0.001$ ) than that in the group of volunteers. The ratio of change in the detectable ducts in the group of patients was significantly lower ( $P = 0.011$ ) than that in the group of volunteers.

**CONCLUSIONS:** Our study suggests that dynamic MR sialographic data in addition to MR sialographic images might be useful for the diagnosis of Sjögren's syndrome.

*Oral Diseases* (2006) 12, 408–414

**Keywords:** dynamic; Sjögren's syndrome; MR sialography; salivary gland; function

## Introduction

Recently, the evaluation of tissue function using various modalities including magnetic resonance (MR) imaging, computed tomography, positron emission tomography, and ultrasound has become more practical in the medical and dental fields (Matos *et al*, 1997; Kats *et al*,

2003; Punwani *et al*, 2003; Ghosh *et al*, 2004; Morimoto *et al*, 2005a; Nakamoto *et al*, 2005; Vaishali *et al*, 2005). In our previous report, we announced 'dynamic MR sialography' as a new non-invasive diagnostic technique for the functional evaluation of salivary glands in their physiologic state (Morimoto *et al*, 2005a). The technique is similar to the dynamic MR cholangiopancreatography (MRCP) technique, in which images are acquired before and after the administration of secretin. The dynamic MRCP technique visualizes the pancreatic ducts in their physiologic state and monitors the ducts filling with saliva in a time-dependent alternation after citric acid stimulation using dynamic MR sialographic images (Matos *et al*, 1997; Kats *et al*, 2003; Punwani *et al*, 2003; Morimoto *et al*, 2005a). We hypothesized that dynamic MR sialography should have the potential to be clinically applied as a diagnostic tool for the many kinds of salivary gland-related diseases (Morimoto *et al*, 2005a).

Among salivary gland-related diseases, one of the most representative diseases is Sjögren's syndrome (Som and Brandwein, 1996; Ohbayashi *et al*, 1998; Tonami *et al*, 1998). It is characterized by xerostomia and keratoconjunctivitis, which result from dysfunction of the salivary and lacrimal glands (Som and Brandwein, 1996). At the present time, X-ray sialography and radionuclide scintigraphy are included as imaging modalities that have been used for the diagnosis of definite Sjögren's syndrome (Som and Brandwein, 1996; Ohbayashi *et al*, 1998; Tonami *et al*, 1998). However, the significance of MR sialographic images as a morphologic examination for the diagnosis of Sjögren's syndrome has been recognized and it is expected that this technique might replace X-ray sialography (Som and Brandwein, 1996; Ohbayashi *et al*, 1998; Tonami *et al*, 1998; Morimoto *et al*, 2002, 2005b).

Therefore, we evaluated the clinical significance of dynamic MR sialographic images and data for patients with Sjögren's syndrome in the present study. We demonstrate that the functional evaluation of salivary glands using dynamic MR sialographic data could be

Correspondence: Dr Y Morimoto, Division of Diagnostic Radiology, Department of Oral Diagnostic Science, Kyushu Dental College, 2-6-1 Manazuru, Kokurakita-ku, Kitakyushu, Fukuoka 803-8580, Japan. Tel: +81 93 582 1131 (ext. 2116, 1331), Fax: +81 93 581 2152, E-mail: rad-mori@kyu-dent.ac.jp  
Received 22 August 2005; revised 17 October 2005; accepted 30 October 2005

more useful than other techniques for the diagnosis of Sjögren's syndrome.

### Subjects and methods

For standardized criteria of dynamic MR sialographic data, we recruited 30 volunteers (15 men and 15 women; mean age, 25.2 years; age range, 22–31 years) with no salivary gland pathology, confirmed both by history and clinical examination. We used the image of a single side of the parotid gland ducts. The side of parotid gland ducts to be imaged was decided in a randomized manner. To get dynamic MR sialographic data from patients with Sjögren's syndrome, we recruited five patients (five women; mean age, 45.2 years; age range, 35–62 years) with definite Sjögren's syndrome satisfying the present criteria (Som and Brandwein, 1996; Fujibayashi, 2004). In brief, in histopathological examinations, positive findings for the invasion of lymphocytes were found in labial mucosa and lacrimal glands. In salivary gland-related examinations, stimulated total salivary flow was lower (< 10 ml in 10 min) and salivary scintigraphy showed delayed uptake, reduced concentration, and/or delayed excretion of tracer. Parotid sialography showed the presence of diffuse sialectasias (punctate, cavitory, or destructive pattern), without evidence of obstruction in the major ducts. In ocular examinations, the Schimer's test result was < 5 mm in 5 min, and the Rose Bengal score was over 3. Another ocular dye score was positive. Regarding the presence of autoantibodies in the serum, antibodies to Ro/SSA antigens, La/SSB antigens, or both were detected. If the results from two of the four kinds of examinations were positive, the patient was considered to have Sjögren's syndrome. We used the image of a single side of the parotid gland ducts, as in the volunteers. The side of parotid gland ducts to be imaged was also decided in a randomized manner unless the main complaint was limited to one side. The study design was approved by the institutional review board of Kyushu Dental College. Informed consent was obtained from all volunteers before the MR examination.

All images were acquired using a 1.5 T full-body MR system (VISART; Toshiba, Tokyo, Japan) with a circular polarized neck coil to visualize the parotid gland ducts (Morimoto *et al*, 2002, 2004, 2005a,b). T1-weighted, T2-weighted, and two-dimensional fast asymmetric spin-echo sequences (2D-FASE) images were acquired for each subject. The MR imaging parameters used are shown in Table 1. Fat saturation suppressed signal from subcutaneous fat. A previously described

method was used for identifying the parotid gland ducts (Morimoto *et al*, 2002, 2004, 2005a,b).

The dynamic MR sialographic images and data were acquired as previously described (Morimoto *et al*, 2000, 2005a). In brief, first, acquisition of the optimal section using 2D-FASE sequencing with single-section acquisition of thick sections was repeated every 30 s (acquisition time: 18 s; interval time: 12 s) before and after a few drops of 5% citric acid were placed on the tongue. Evaluation of the time-dependent increases or decreases in the area of the detectable parotid gland's main ducts, high-intensity linear structures from the parotid glands to the upper first molar region, before and after citric acid stimulation was precisely visualized every 30 s and analyzed from the MR sialographic images (Figures 1a and 2a). Simultaneously, the time from the end of citric acid stimulation to the occurrence of the maximum area of the ducts was measured. This dynamic procedure was conducted during the 8 min after stimulation. The time it took for the parotid gland duct area to return to 50% of its pre-citric acid stimulation level was measured. Evaluation of the time-dependent alternation associated with citric acid stimulation of the area of the detectable parotid gland ducts was quantitatively measured using the scanner-computer analysis system (Morimoto *et al*, 2000, 2005a).

For each subject, a graph was drawn to demonstrate the relationship between the time course after citric acid stimulation and the changing ratio of the detectable area in the parotid gland ducts. The changing ratio was determined as follows: changing ratio = detectable area of parotid gland ducts/minimum detectable area.

As the morphological finding on MR sialographic images of patients, we evaluated whether or not the so-called 'apple-tree-like appearance' was depicted, and the likely characteristic radiologic findings of Sjögren's syndrome on X-ray sialographic images (Som and Brandwein, 1996; Ohbayashi *et al*, 1998; Tonami *et al*, 1998; Kalinowski *et al*, 2002; Morimoto *et al*, 2002, 2004; Baur *et al*, 2004). In concrete, the presence or absence of diffuse areas of punctate high signal intensity 1 mm or less in diameter on MR sialographic images were evaluated (Som and Brandwein, 1996).

Student's *t*-test was used to examine the differences between the volunteers' group and the patients' group on the following: (1) maximum area of the detectable parotid gland ducts before and after citric acid stimulation; (2) changing ratio; (3) time from the end of citric acid stimulation to the occurrence of the maximum area of the detectable parotid gland ducts; and (4) time it took for the parotid gland ducts to decrease from their

**Table 1** Magnetic resonance imaging parameters

Sequence	TR/TE/FA/ETL	Thickness (mm)	Matrix	Acquisition time (min:s)	FOV (mm)
T1WI	500/15/90/37	6	224 × 320	3:30	200 × 200
T2WI	3500/108/90/27	6	224 × 256	3:30	200 × 200
2D-FASE	6000/500/90/148	30–60	512 × 512	0:18	200 × 200

TR, (Time of Repetitions); TE, (Time of Echo); FA, (Flip Angle); ETL, (Echo-train length); FOV, (Field of View); T1WI, T1-weighted image; T2WI, T2-weighted image; 2D-FASE, two-dimensional fast asymmetric spin-echo sequences.

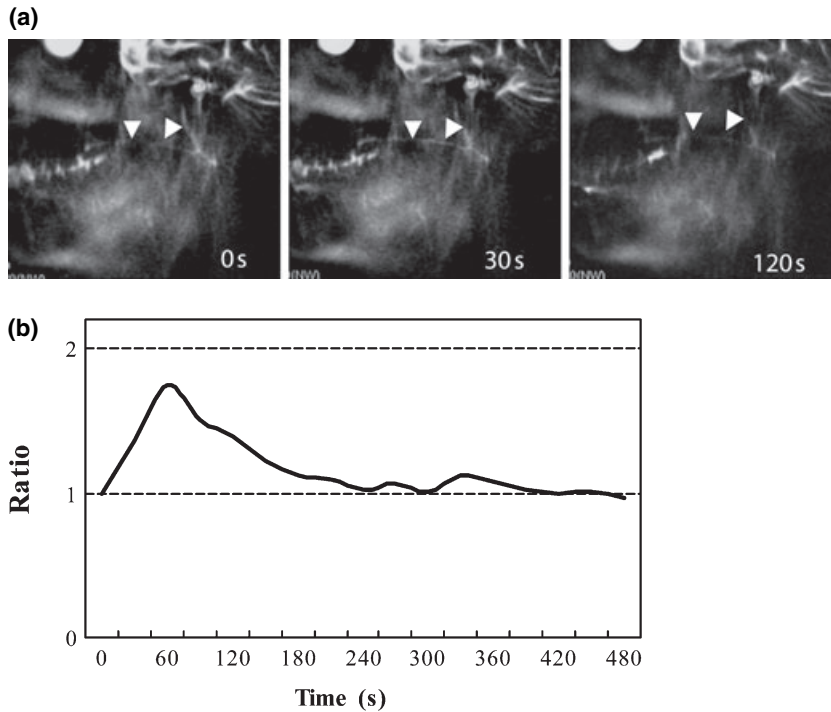


**Figure 1** Dynamic magnetic resonance sialographic images and data using 2D-FASE from the right parotid gland ducts of a 30-year-old healthy male volunteer. (a) The main duct and its side branches become clearer in a time-dependent fashion immediately after citric acid stimulation until 30 s (arrowheads). After 30 s, the main duct becomes more obscure in a time-dependent manner (arrowheads). (b) Graph demonstrating the relationship between the time course after citric acid stimulation and the changing ratio of the detectable parotid gland duct area for the subject in (a)

maximum level to the 50% level of pre-citric acid stimulation.  $P < 0.05$  was considered statistically significant.

## Results

Representative dynamic MR sialographic images and graphs obtained in healthy volunteers are shown in Figure 1. The main duct became clearer in a time-dependent fashion from immediately after citric acid stimulation until 30-60 s poststimulation. Thereafter, the main duct became more obscure in a time-dependent manner (Figure 1a). In the graph demonstrating the relationship between the time course and the changing ratio of the detectable area in the ducts, the changing ratio at first increases in the first 30 s in a time-dependent manner, and then decreases after the first 30 s in a time-dependent fashion (Figure 1b).

Typical dynamic MR sialographic images and graphs obtained from patients with definite Sjögren's syndrome are shown in Figure 2. A small amount of atrophy of the left parotid duct was visible along its entire length, and diffuse areas of punctate high signal intensity 1 mm or less in diameter, giving the so-called 'apple-tree-like appearance', were displayed on dynamic MR sialographic images of pre-citric acid stimulation (Figure 2a) as well as those on plain film X-ray sialographs (Figure 2b). Even after citric acid stimulation, these findings remained unchanged (Figure 2a). Therefore, in the graph demonstrating the relationship between the time course and the changing ratio of the detectable area in the ducts, the changing ratio at first increases in a time-dependent manner, and then remains almost unchanged even

between pre- and post-citric acid stimulation, unlike in healthy volunteers (Figure 2b).

The volunteers' and patients' data are summarized in Tables 2 and 3. Regarding the maximum area of parotid gland ducts before and after citric acid stimulation without a small amount of atrophy of the parotid gland ducts along the gland's entire length, the analysis using Student's *t*-test revealed a significant difference between the two groups on the maximum area before ( $P < 0.001$ ) and after ( $P = 0.011$ ) citric acid stimulation, and the maximum area of the volunteers was significantly larger than that of the patients. With a small amount of atrophy of the parotid gland ducts, however, there was no significant difference between the two groups ( $P = 0.056$ ). On the maximum changing ratio, the analysis using Student's *t*-test revealed a significant difference between the two groups ( $P < 0.001$ ), and the maximum changing ratio of the volunteers was significantly bigger than that of the patients. There was no significant difference between the two groups on the time to occurrence of the maximum duct area after stimulation ( $P = 0.064$ ) and on the time it took for the detectable duct area to return to nearly 50% of its former area ( $P = 0.155$ ) using Student's *t*-test.

## Discussion

In a previous study, we reported a new technique for the evaluation of parotid gland function using dynamic MR sialography before and after citric acid stimulation (Morimoto *et al*, 2005a). In that report, we hypothesized that some parameters in the technique, including the detectable ductal area and changing ratio, could be

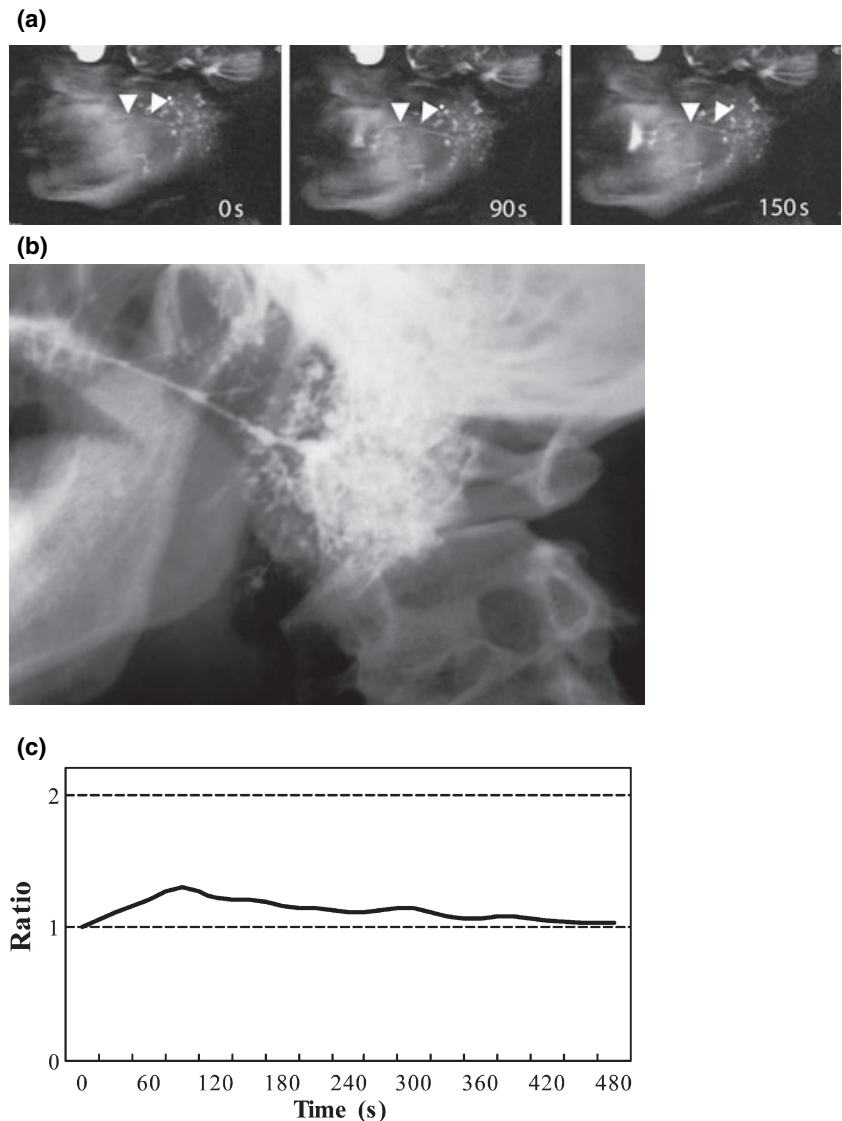


**Figure 2** Dynamic magnetic resonance (MR) sialographic images and data using 2D-FASE from the left parotid gland ducts of a 60-year-old female with definite Sjögren's syndrome. **(a)** The so-called 'apple-tree-like appearance' is shown on dynamic MR sialographic images of pre-and post-citric acid stimulation. The main duct and its side branches become a little clearer in a time-dependent fashion immediately after citric acid stimulation until 90 s (arrowheads). After 90 s, the main duct becomes more obscure in a time-dependent manner. The detectable areas in the main duct and the side branches before and after citric acid stimulation are relatively unchanged. **(b)** Entire X-ray sialographic image of the patient shown in **(a)** the same to MR sialographic images. **(c)** Graph demonstrating the relationship between the time course after citric acid stimulation and the changing ratio of the detectable area in the parotid gland ducts for the subject in **(a)**. The changing ratio is significantly lower than that in the volunteers

**Table 2** Parameters in dynamic magnetic resonance sialography of parotid gland ducts in the subjects ( $n = 30$ )

<i>Maximum area (mm<sup>2</sup>) of parotid gland ducts</i>		<i>Maximum changing ratio to before citric acid stimulation</i>	<i>Period (s) to occurrence of maximum area</i>	<i>Period (s) to return to its pre-citric acid stimulation 50% level</i>
<i>Before citric acid stimulation</i>	<i>After citric acid stimulation</i>			
299 ± 163 (80–640)	506 ± 236 (191–882)	1.80 ± 0.43 (1.15–2.45)	65.2 ± 29.5 (30–150)	139.6 ± 71.6 (60–240)

Values are mean ± SD (range).

useful as diagnostic tools for various salivary gland-related diseases (Morimoto *et al*, 2005a). In the present study, we determined whether dynamic MR sialographic images and data would be useful as a diagnostic tool for definite Sjögren's syndrome.

The most interesting result in the present study is the significant difference of the number in the maximum changing ratio between volunteers and patients with definite Sjögren's syndrome. The changing ratio in dynamic parameters significantly correlated with functional evaluation, and might be the most important parameter of

salivary function (Morimoto *et al*, 2005a). With 1 standard deviation (SD) as the abnormal level of the maximum changing ratio, the status of all five patients (true positive = 100%) was diagnosed as abnormal and the status of no volunteer was misdiagnosed (false negative = 0%). Therefore, this functional parameter (maximum changing ratio) is clearly valid as a diagnostic criterion for Sjögren's syndrome as shown by the present data. In addition, the so-called 'apple-tree-like structures' in all patients were depicted as typical morphologic findings as well as on plain X-ray sialographs, but were

**Table 3** Parameters in dynamic magnetic resonance sialography in the patients with definite Sjögren's syndrome

Patient no.	Age (years)	Gender	Side	Maximum area (mm <sup>2</sup> ) of parotid gland ducts		Maximum changing ratio to before citric acid stimulation	Period (s) to occurrence of maximum area	Period (s) to return to its pre-citric acid stimulation 50% level
				Before citric acid stimulation	After citric acid stimulation			
1	55	F	L	29 (348)	49 (392)	1.7 (1.1)	90	180
2	71	F	R	38 (311)	47 (331)	1.2 (1.1)	90	270
3	47	F	R	62 (456)	84 (492)	1.4 (1.1)	120	270
4	53	F	L	74 (537)	93 (602)	1.3 (1.1)	90	150
5	59	F	R	79 (473)	81 (481)	1.0 (1.0)	60	90
	57 ± 8.9 <sup>a</sup>			56.4 ± 22.0 (425 ± 93.2)	70.8 ± 21.2 (459 ± 103)	1.32 ± 0.26 (1.08 ± 0.04)	90 ± 21.2	192 ± 78.2

<sup>a</sup>Mean ± SD. The numbers in brackets show maximum detectable ductal areas with diffuse areas of punctate high signal and maximum changing ratio, before citric acid stimulation using the maximum detectable ductal areas.

not seen in all volunteers (Som and Brandwein, 1996; Ohbayashi *et al*, 1998; Tonami *et al*, 1998, 2001; Becker *et al*, 2000; Kalinowski *et al*, 2002; Morimoto *et al*, 2002, 2004; Baur *et al*, 2004). If an improvement in image quality is needed for morphological examination, we can acquire the MR sialographic images using 3D-FASE sequences before obtaining the dynamic MR sialography without inconvenience (Morimoto *et al*, 2002, 2004, 2005b). Therefore, dynamic MR sialography could examine both morphological and functional features of Sjögren's syndrome at the same time. Until now, if both parameters are needed as diagnostic criteria for Sjögren's syndrome, both X-ray sialographic and scintigraphic data had to be used (Som and Brandwein, 1996; Ohbayashi *et al*, 1998; Tonami *et al*, 1998; Morimoto *et al*, 2002, 2004; Baur *et al*, 2004).

In other words, MR imaging is invariably needed to examine the condition of the salivary glands in pathological states including Sjögren's syndrome (Som and Brandwein, 1996). If dynamic MR sialography were then added, the morphological and functional evaluation of the salivary glands could be achieved at the same time. The practical application of dynamic MR sialographic imaging is more useful than other methods because it allows the easy non-invasive evaluation of each salivary gland without patient inconvenience (Som and Brandwein, 1996; Ohbayashi *et al*, 1998; Tonami *et al*, 1998, 2001; Becker *et al*, 2000; Kalinowski *et al*, 2002; Morimoto *et al*, 2002, 2004, 2005a; Baur *et al*, 2004). Furthermore, to evaluate the amount of saliva coming from a particular salivary gland presently requires cannulation of its duct, with attendant pain to the patient (Enfors, 1962). Salivary scintigraphy using <sup>99m</sup>TcO<sub>4</sub><sup>-</sup> requires a special room for handling the radioisotope and venipuncture for injection of the <sup>99m</sup>TcO<sub>4</sub><sup>-</sup> solution (Som and Brandwein, 1996; Tonami *et al*, 2001; Baur *et al*, 2004).

In all five patients in the present study, the present diagnostic criteria of definite Sjögren's syndrome were satisfied (Som and Brandwein, 1996; Tonami *et al*, 2001). Radiological findings on X-ray sialographic images of all five patients were classified as point or round type, and the so-called 'apple-tree-like appearances' were shown on all MR sialographic images (Som and Brandwein, 1996; Ohbayashi *et al*, 1998; Tonami *et al*, 1998; Kalinowski *et al*, 2002; Morimoto *et al*, 2002, 2004; Baur *et al*, 2004). Diffuse areas of punctate high signal intensity 1 mm or less in diameter on MR sialographic images demonstrate the small amount of atrophy of the parotid gland ducts and branches (Som and Brandwein, 1996). The regions should almost not work as ducts of salivary excretion (Som and Brandwein, 1996). Therefore, we were perplexed as to whether diffuse areas of punctate high signal intensity 1 mm or less in diameter should be included in the maximum detectable ductal areas as one of the dynamic parameters. The maximum detectable ductal areas in dynamic parameters significantly correlated with total saliva volume, and might be important as one parameter of the salivary function (Morimoto *et al*, 2005a). Maximum detectable ductal areas with and without diffuse

areas of punctate high signal were analyzed in the present study because we wanted to judge the effective use of dynamic MR sialography for the diagnosis of Sjögren's syndrome. Regarding the maximum detectable ductal areas without diffuse areas of punctate high signal intensity, the analysis using Student's *t*-test revealed a significant difference between volunteers and patients with Sjögren's syndrome; however, no difference was found regarding the maximum detectable ductal areas with diffuse areas of punctate high signal intensity. The present results suggest that the maximum detectable ductal areas without diffuse areas of punctate high signal intensity might be preferential for the diagnosis of Sjögren's syndrome.

Conversely, given that the cases of all patients in the present study were classified as the point or round type on X-ray sialographic images, there might be no significant difference between volunteers and patients regarding the maximum detectable ductal areas with diffuse areas of punctate high signal intensity. If patients with the cavity or destruction type of cases of Sjögren's syndrome were included among the subjects, their data probably would have been significantly different from the data of both the volunteers and the patients with the point or round type of cases. Therefore, diffuse areas of punctate high signal intensity 1 mm or less in diameter could not be found on X-ray sialographic findings in patients with the cavity or destruction type of cases due to the destruction of the small amount of atrophy of the parotid gland ducts and branches (Som and Brandwein, 1996; Ohbayashi *et al*, 1998). We speculated that the maximum detectable ductal area with diffuse areas of punctate high signal intensity might indicate an advanced degree of Sjögren's syndrome. Further studies are needed to prove this.

Regarding other parameters, the time to occurrence of the maximum duct area after stimulation and the time it took for the detectable duct area to return to nearly 50% of its former area, the times in patients with definite Sjögren's syndrome were longer than those in volunteers, but their utility for the diagnosis of definite Sjögren's syndrome could not be demonstrated.

The need for 30 s per one dynamic MR sialographic image and data set was the most limiting point of our technique using dynamic MR sialography. Our present technique could not detect a relatively small dysfunction in the salivary gland except in patients with larger functional changes. However, we are convinced that improvement in our sequences by shortening the acquisition time could be effective for the diagnosis of Sjögren's syndrome.

One possible limitation of our present study is that the sample size was small. The variables of race and sex could not be studied from our study sample. At the same time, the age of our control group did not match that of the experimental group. As persons age, their stimulating saliva flow rate should be lower. Therefore, our results regarding the differences in some parameters between the two groups should be judged as relatively lower. Therefore, larger sample sizes should be studied to establish the diagnostic criteria of each parameter for

definite Sjögren's syndrome. In addition, dynamic MR sialography should be tried in patients with various kinds of salivary gland-related diseases including dry mouth, Sjögren's syndrome, chronic sialoadenitis, acute sialoadenitis, salivary gland duct stones, and ranula. Applying this technique to many patients with different salivary gland-related diseases would make it possible to identify different patterns of diseases. Thus, we expect that each salivary gland-related disease could someday be diagnosed from its particular graph pattern.

### Acknowledgements

This study was supported in part by grants from the Grant in Aid for Scientific Research from the Ministry of Education, Science, Sports and Culture of Japan, and a grant-in-aid for scientific research from the President of the Kyushu Dental College, Kitakyushu, to YM.

### References

- Baur DA, Heston TF, Helman JI (2004). Nuclear medicine in oral and maxillofacial diagnosis: a review for the practicing dental professional. *J Contemp Dent Pract* **15**: 94–104.
- Becker M, Marchal F, Becker CD *et al* (2000). Sialolithiasis and salivary ductal stenosis: diagnostic accuracy of MR sialography with a three-dimensional extended-phase conjugate-symmetry rapid spin-echo sequence. *Radiology* **217**: 347–358.
- Enfors BO (1962). The parotid and submandibular secretion in man. Quantitative recordings of the normal and pathological activity. *Acta Otolaryngol* **172**: 1–67.
- Fujibayashi T (2004). Revised Japanese criteria for Sjögren's syndrome (1999): availability and validity. *Mod Rheumatol* **14**: 425–434.
- Ghosh N, Tampieri D, Melancon D (2004). Immediate evaluation of angioplasty and stenting results in supra-aortic arteries by use of a Doppler-tipped guidewire. *Am J Neuroradiol* **25**: 1172–1176.
- Kalinowski M, Heverhagen JT, Rehberg E *et al* (2002). Comparative study of MR sialography and digital subtraction sialography for benign salivary gland disorders. *Am J Neuroradiol* **23**: 1485–1492.
- Kats J, Kraai M, Dijkstra AJ *et al* (2003). Magnetic resonance cholangiopancreatography as a diagnostic tool for common bile duct stones: a comparison with ERCP and clinical follow-up. *Dig Surg* **20**: 32–37.
- Matos C, Metens T, Deviere J *et al* (1997). Pancreatic duct: morphologic and functional evaluation with dynamic MR pancreatography after secretin stimulation. *Radiology* **203**: 435–441.
- Morimoto Y, Tanaka T, Kito S *et al* (2000). Quantitative radiographic changes in the mandible and the tibia in systematically loaded rats fed a low-calcium diet. *Oral Dis* **6**: 310–317.
- Morimoto Y, Tanaka T, Yoshioka I *et al* (2002). Virtual endoscopic view of salivary gland ducts using MR sialography data from three dimension fast asymmetric spin-echo (3D-FASE) sequences: a preliminary study. *Oral Dis* **8**: 268–274.
- Morimoto Y, Tanaka T, Tominaga K *et al* (2004). Clinical application of MR sialographic 3D-reconstruction imaging and MR virtual endoscopy for salivary gland duct analysis. *J Oral Maxillofac Surg* **62**: 1236–1244.

- Morimoto Y, Ono K, Tanaka T *et al* (2005a). The functional evaluation of salivary glands using dynamic MR sialography following citric acid stimulation: a preliminary study. *Oral Surg Oral Med Oral Pathol Oral Radiol Endod* **100**: 357–364.
- Morimoto Y, Tanaka T, Kito S *et al* (2005b). Utility of three dimension fast asymmetric spin-echo (3D-FASE) sequences in MR sialographic sequences: model and volunteer studies. *Oral Dis* **11**: 35–43.
- Nakamoto Y, Tatsumi M, Hammoud D *et al* (2005). Normal FDG distribution patterns in the head and neck: PET/CT evaluation. *Radiology* **234**: 879–885.
- Ohbayashi N, Yamada I, Yoshino N *et al* (1998). Sjögren syndrome: comparison of assessments with MR sialography and conventional sialography. *Radiology* **209**: 683–688.
- Punwani S, Gillams AR, Lees WR (2003). Non-invasive quantification of pancreatic exocrine function using secretin-stimulated MRCP. *Eur Radiol* **13**: 273–276.
- Som PM, Brandwein M (1996). Salivary glands. In: Som PM, Curtin HD, eds. *Head and neck imaging*, 3rd edn. St Louis, MO: Mosby, pp. 823–914.
- Tonami H, Ogawa Y, Matoba M *et al* (1998). MR sialography in patients with Sjögren syndrome. *Am J Neuroradiol* **19**: 1199–1203.
- Tonami H, Higashi K, Matoba M *et al* (2001). A comparative study between MR sialography and salivary gland scintigraphy in the diagnosis of Sjögren syndrome. *J Comput Assist Tomogr* **25**: 262–268.
- Vaishali C, Marion H, Linda S *et al* (2005). Transient neurologic deficit after acetazolamide challenge for computed tomography perfusion imaging. *J Comput Assist Tomogr* **29**: 278–280.

Copyright of Oral Diseases is the property of Blackwell Publishing Limited and its content may not be copied or emailed to multiple sites or posted to a listserv without the copyright holder's express written permission. However, users may print, download, or email articles for individual use.